

# SCIENTIFIC REPORTS



OPEN

## Self-sorting heterodimeric coiled coil peptides with defined and tuneable self-assembly properties

Christopher Aronsson<sup>1</sup>, Staffan Dånmark<sup>1</sup>, Feng Zhou<sup>2</sup>, Per Öberg<sup>3,†</sup>, Karin Enander<sup>1</sup>, Haibin Su<sup>2</sup> & Daniel Aili<sup>1</sup>

Received: 16 June 2015

Accepted: 17 August 2015

Published: 15 September 2015

Coiled coils with defined assembly properties and dissociation constants are highly attractive components in synthetic biology and for fabrication of peptide-based hybrid nanomaterials and nanostructures. Complex assemblies based on multiple different peptides typically require orthogonal peptides obtained by negative design. Negative design does not necessarily exclude formation of undesired species and may eventually compromise the stability of the desired coiled coils. This work describes a set of four promiscuous 28-residue de novo designed peptides that heterodimerize and fold into parallel coiled coils. The peptides are non-orthogonal and can form four different heterodimers albeit with large differences in affinities. The peptides display dissociation constants for dimerization spanning from the micromolar to the picomolar range. The significant differences in affinities for dimerization make the peptides prone to thermodynamic self-sorting as shown by thermal unfolding and fluorescence experiments, and confirmed by simulations. The peptides self-sort with high fidelity to form the two coiled coils with the highest and lowest affinities for heterodimerization. The possibility to exploit self-sorting of mutually complementary peptides could hence be a viable approach to guide the assembly of higher order architectures and a powerful strategy for fabrication of dynamic and tuneable nanostructured materials.

The coiled coil is one of the most abundant protein structural motifs found in nature. It is especially common in fibrous proteins such as myosin, keratin and fibrinogen<sup>1</sup>. Computational analysis has established that about 3% of all amino acids in the known genomes are involved in coiled coil structures<sup>2</sup>. As reported by Crick, Pauling and Corey in the 1950's, coiled coils can be described as two or more  $\alpha$ -helices that intertwine, creating rope-like structures<sup>1,3</sup>. The amino acid sequence of coiled coils typically show a heptad repetition of hydrophobic (**h**) and polar (**p**) residues in a **hpphppp** pattern, commonly denoted as  $(abcdefg)_n$  where  $n$  is the number of repeats and  $a$ - $g$  show the relative positions of the amino acids in a helical wheel diagram (Fig. 1). The hydrophobic effect is the main driving force for association and folding of coiled coils. Hydrophobic residues at  $a$  and  $d$  positions pack together in a “knobs-into-hole” fashion to minimize their interaction with water molecules<sup>1</sup>. The stability of coiled coils is also affected by the presence of charged residues at  $e$  and  $g$  positions. Oppositely charged residues stabilize inter-helical arrangements whereas like charges lead to repulsion and destabilization. The heptad repeat pattern makes coiled coils fairly straightforward to de novo design and design rules have been extensively investigated, as summarized in several review articles<sup>4-8</sup>.

Heterodimeric coiled coils with tuneable and well-defined assembly properties are of great interest as model systems to mimic and study biomolecular interactions involved in for example vesicle fusion<sup>9</sup>, and cell-signalling events<sup>10</sup>. Coiled coils have also been exploited as components in a range of supramolecular

<sup>1</sup>Division of Molecular Physics, Department of Physics, Chemistry and Biology, Linköping University, 581 83 Linköping, Sweden. <sup>2</sup>School of Materials Science and Engineering, Nanyang Technological University, Singapore 639798. <sup>3</sup>Vehicular Systems, Department of Electrical Engineering, Linköping University, 581 83 Linköping, Sweden. <sup>†</sup>Present address: Wolfram MathCore, Teknikringen 1F, 583 30 Linköping, Sweden. Correspondence and requests for materials should be addressed to D.A. (email: daniel.aili@liu.se)

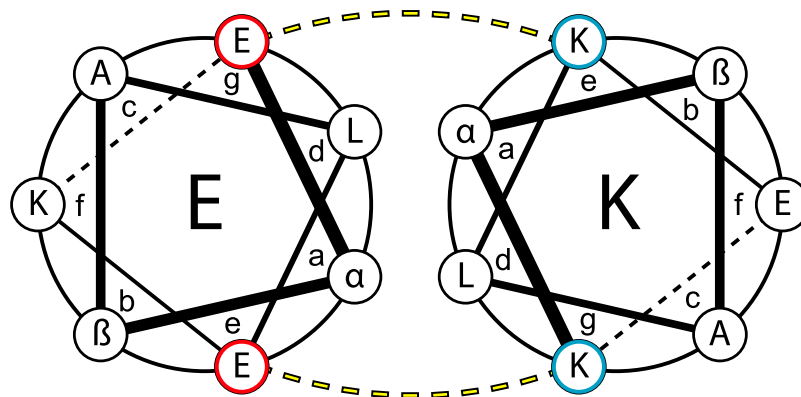


**Figure 1.** A helical wheel diagram showing the coiled coil heptad repeat for a heterodimer. Residues at *a* and *d* creates a hydrophobic core while *e* and *g* residues favours heterodimerization through formation of stabilizing salt bridges. For peptides used in this work,  $\alpha$  = Val or Ile (3<sup>rd</sup> heptad Asn),  $\beta$  = Ala or Ser.

materials, including peptide-polymer hybrid hydrogels<sup>11,12</sup>, peptide fibers<sup>13</sup>, and peptide-nanoparticle hybrids<sup>14</sup>. Assembly of complex peptide nanostructures require simultaneous use of multiple peptides that displays a varying degree of complementarity. Recent beautiful examples include the assembly of a peptide tetrahedron by Jerala *et al.*<sup>15</sup>, based on six different orthogonal coiled coil forming peptide pairs, as well as a number of complex but structurally well-defined nanostructured assemblies described by Woolfson *et al.*<sup>16</sup>.

To be able to control the self-assembly process and stability of peptide-based supramolecular nanostructures, it is critical to have tuneable and quantified affinities for oligomerization<sup>17</sup>. Several different strategies have been developed to obtain coiled coils with defined oligomeric states, helix orientations and affinities for association<sup>18–20</sup>. The length of a peptide greatly affects its potential to interact with other peptides. Increasing the number of heptads typically increases the affinity for oligomerization. Recently, Thomas *et al.* described a set of heterodimeric coiled coils with tuneable and quantified dissociation constants in the micromolar to sub-nanomolar range obtained by varying the numbers of heptad repeats<sup>21</sup>. Although highly successful for tuning the interaction strength the use of peptides of different length in the same coiled coil motif may result in problems with fringing and unspecific interactions caused by the overhanging ends.

In order to reduce unwanted interactions and to prevent formation of undesired folded species, negative design elements are typically introduced. Commonly, polar or charged amino acids at *a* or *d* or a pinpointed charge interaction at specific *e* and *g* positions, are introduced<sup>22–24</sup>. Efforts to reduce formation of undesired oligomers and folds may however result in an overall decrease in stability of the intended structures. In contrast, by positive design, desired species are favoured by introducing stabilizing elements. The unwanted species can still form but the equilibrium is shifted towards the thermodynamically most stable structures. Example of positive design elements for coiled coils are to include more hydrophobic residues at *a* and *d*<sup>25</sup>.

Here, we investigate the possibility to form specific heterodimers with high fidelity from mixtures of complementary peptides based on large differences in affinities. We describe a set of four peptides capable of forming parallel heterodimeric coiled coils with dissociation constants spanning from low micromolar to the picomolar range. The affinity for dimerization was modulated using the well-known differences in packing efficiencies of the two  $\beta$ -branched amino acids valine and isoleucine in the hydrophobic core and the difference in  $\alpha$ -helical propensities of serine and alanine<sup>25</sup>. Using this strategy we obtained four rather similar 28-residue peptides that can be combined into four different parallel heterodimeric coiled coils. The conformations and stabilities were investigated using circular dichroism (CD) spectroscopy and molecular dynamics (MD) simulations. When all peptides were combined, the large differences in dissociation constants promoted social self-sorting and assembly of only two of the four possible coiled coils. The possibility to exploit self-sorting of mutually complementary peptides to guide the assembly of higher order architectures is an interesting alternative to the use of orthogonal peptides that further enables fabrication of dynamic and tuneable materials and nanostructures.

## Results and Discussion

**Peptide design.** Four different 28 amino acid residue coiled coil forming peptides (EV, EI, KV, KI) were developed (Table 1) following established coiled coil design rules<sup>26</sup>. The sequences were based upon peptides designed by Hodges *et al.*<sup>20,25</sup>, and Woolfson *et al.*<sup>21</sup>, but with some modifications in order to obtain two sets of complementary peptides with large differences in affinities for dimerization. In short, the peptides were designed to heterodimerize at neutral pH by adding complementarily charged residues at *e* and *g* using glutamic acid (Glu, E) for EV and EI and lysine (Lys, K) for KV and KI. The hydrophobic

	<i>gabcdef</i>	<i>gabcdef</i>	<i>gabcdef</i>	<i>gabcdef</i>
EV	EVSALEK	EVSALEK	ENSALEW	EVSALEK
KV	KVSALKE	KVSALKE	KNSALKW	KVSALKE
EI	EIAALEK	EIAALEK	ENAALEW	EIAALEK
KI	KIAALKE	KIAALKE	KNAALKW	KIAALKE

**Table 1. Peptide sequences with corresponding heptad register.**

face of the helices has leucine (Leu, L) at position *d* and a  $\beta$ -branched amino acid at position *a*. Valine (Val, V) was used at position *a* for EV and KV peptides whereas isoleucine (Ile, I) was included at this position for EI and KI. These amino acids were chosen in order to obtain a wide span of affinities for dimerization for the four possible combinations of coiled coil heterodimers (EVKV, EVKI, EIKV and EIKI). An asparagine (Asn, N) residue was incorporated at *a* in the third heptad in all peptides to promote formation of dimeric structures with parallel orientation<sup>21,26</sup>. The asymmetric positioning of the polar Asn in the hydrophobic core will also favour assembly of in-register structures because of favourable Asn-Asn' pairing between two peptides. The helix promoting amino acid alanine (Ala, A) was used at position *b* in all peptides and at position *c* in the EI and KI peptides. In the EV and KV peptides, position *c* was instead occupied by serine (Ser, S) that has slightly lower  $\alpha$ -helix propensity compared to Ala. To balance the net charge of the peptides and to increase water solubility Glu residues were included at position *f* for the KV and KI. For EV and EI, Lys was used instead. In the third heptad a tryptophan (Trp, W) was incorporated at *f* as a chromophore.

**Peptide characterization.** The peptides were synthesized on solid support using Fmoc chemistry and their secondary structure and folding properties were characterized using CD spectroscopy. CD spectra of the individual peptides showed that the peptides were mainly random coils at neutral pH (Fig. 2a). This indicates that the charge repulsion provided by residues at *e* and *g* was sufficient to prevent homodimerization and folding. A slight shift of the negative band from 198 nm in the spectra for EV and KV to 201–202 nm for EI and KI indicate that the latter two may exhibit a small amount of secondary structure. This is presumably because Ile is slightly more hydrophobic compared to Val but also provides a better packing of the hydrophobic core<sup>20</sup>. It should also be noted that the negative band shift is slightly more pronounced for KI than for EI. This can be explained by the longer and more flexible side chain in Lys compared to Glu. The  $\epsilon$ -amino groups in neighbouring Lys residues can be positioned further apart as compared to the  $\gamma$ -carboxyls in two adjacent Glu residues. A lower charge repulsion between KI monomers than between EI monomers is thus expected. A similar tendency has been observed for Fos-Jun heterodimers that also can form Jun-Jun homodimers<sup>27</sup>.

Thermal denaturation experiments showed that only a moderate increase in temperature abolished all tendencies of folding for EI and KI (Fig. 2b, Supplementary Table S1). This clearly indicates that the interactions between peptides of the same kind are very dynamic and unstable with melting temperatures ( $T_m$ ) lower than 20 °C. By changing the pH closer to the pI of the individual peptides it is possible to trigger homooligomerization and folding of the peptides (Supplementary Figure S1, Table S2). The EI and KI homooligomers showed impressive thermal stabilities with  $T_m > 85$  °C, whereas EV had a  $T_m$  of 67 °C. KV did only show minor tendencies to associate with  $T_m$  of <30 °C.

Mixing the different monomers at pH 7 generated CD spectra with two minima at 208 and 222 nm for all four possible heterodimer combinations, indicating formation of  $\alpha$ -helical structures (Fig. 2c). The ratio of the two minima ( $[\Theta]_{222}/[\Theta]_{208}$ ) provides an estimate of the extent of coiled coil formation<sup>28</sup>. A ratio >1 indicates well-defined coiled coils whereas lower values indicate a less defined coiled coil structure. EVKV had the lowest ratio (0.85) whereas EIKI showed the highest ratio (1.01). EVKI and EIKV did also display relatively high  $[\Theta]_{222}/[\Theta]_{208}$  ratios, 0.94 and 0.97 respectively. Addition of 50 vol% of 2,2,2-Trifluoroethanol (TFE), a compound that disrupts hydrophobic cores of coiled coils while maintaining the  $\alpha$ -helical conformation of individual peptides, resulted in a decrease in the  $[\Theta]_{222}/[\Theta]_{208}$  ratio for all dimers (Supplementary Figure S2). For EVKV this decrease was fairly small, from 0.85 to 0.83. For EVKI and EIKV the ratio decreased to 0.84 while the ratio for EIKI decreased to 0.85. All dimers, except EVKV, hence showed a significant change in the  $[\Theta]_{222}/[\Theta]_{208}$  ratio upon addition of TFE. This indicates that these peptide combinations do form defined and stable coiled coils.

Thermal denaturation experiments showed a distinct difference in stability of the different heterodimers (Fig. 2d). EVKV, EVKI and EIKV all demonstrated true monophasic sigmoidal melting curves, indicating discrete and cooperatively folded structures. EIKI did also show this trend in the measureable temperature range (<90 °C) but the peptide did not unfold completely even at the highest temperatures.  $T_m$  ranged from 37 to 87 °C for the different pairs where EVKV and EIKI showed the lowest and the highest  $T_m$  values, respectively (Table 2). An isobestic point at 203 nm was also seen for all heterodimers further indicating that there indeed was a discrete unfolding from  $\alpha$ -helices to random coil (Supplementary Figure S3)<sup>29</sup>.

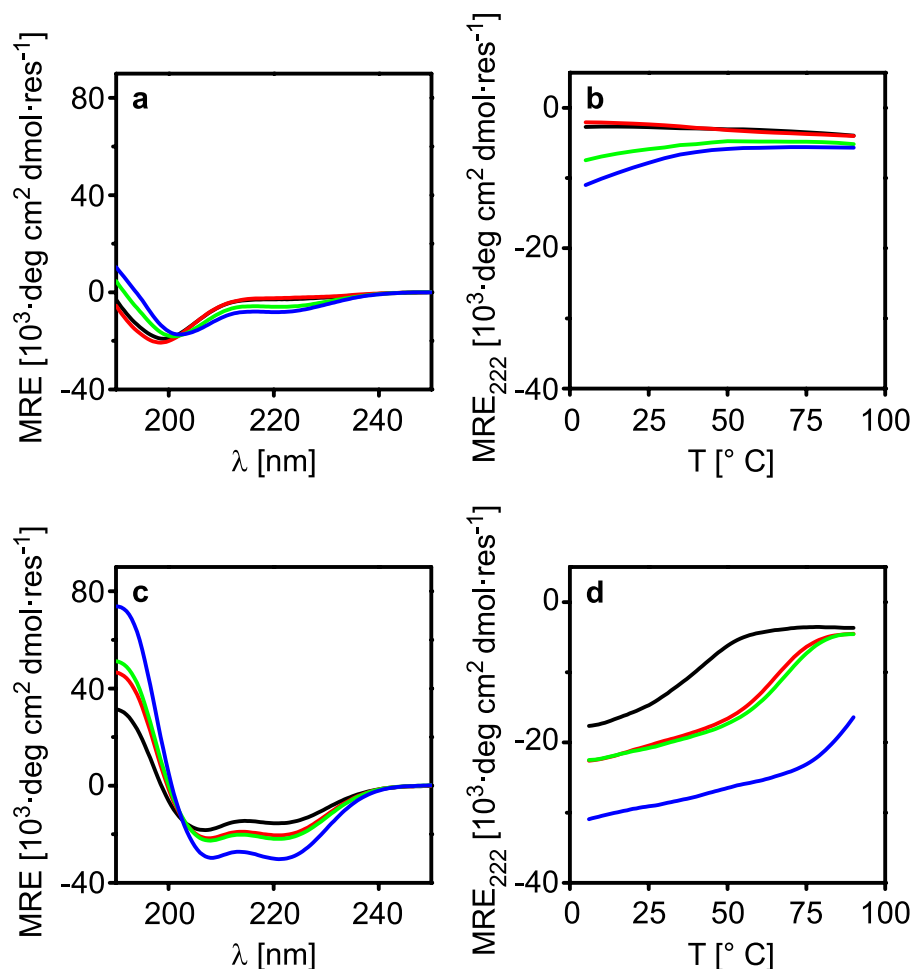


**Figure 2.** CD spectra of (a) monomers at 20°C (b) monomer thermal denaturation (c) coiled coils at 20°C (d) coiled coils thermal denaturation. Key: (a,b) EV = black; KV = red; EI = green; KI = blue. (c,d) EVKV = black; EVKI = red; EIKV = green; EIKI = blue.

	[ $\Theta$ ] <sub>222</sub> at 20°C [ $10^3 \cdot \text{deg cm}^2 \text{ dmol} \cdot \text{res}^{-1}$ ]	[ $\Theta$ ] <sub>222</sub> /[ $\Theta$ ] <sub>208</sub> at 20°C		T <sub>m</sub> [°C]	K <sub>d</sub> [M] at 20°C
		PB	TFE		
EVKV	-15.4	0.85	0.83	37.4 ± 0.1	1.4 ± 1.5 × 10 <sup>-6</sup>
EVKI	-20.4	0.94	0.84	61.6 ± 0.4	8.5 ± 7.1 × 10 <sup>-8</sup>
EIKV	-21.8	0.97	0.84	63.7 ± 0.5	7.2 ± 4.7 × 10 <sup>-8</sup>
EIKI	-30.1	1.01	0.85	86.7 ± 0.04	< 1.0 × 10 <sup>-10</sup> (0.43 ± 4.9 × 10 <sup>-16</sup> )*

**Table 2.** CD characterization data for the different heterodimers. \*Calculated value

The method of continuous variation was utilized to examine the oligomerization state of the coiled coils. The molar ratio of each monomer was varied and the ellipticity at [ $\Theta$ ]<sub>222</sub> was measured for all ratios (Supplementary Figure S4). This confirmed that all four peptide combinations primarily associate in a 1:1 ratio. Formation of dimers was verified using several predictive analysing tools, including Logiccoil<sup>30</sup>, RFCoil<sup>31</sup>, and ProCoil<sup>32</sup>.

Formation of transient or less stable oligomers can however not be fully excluded but MD simulations further supported formation of stable parallel heterodimers for all peptides pairs. Within 40 ns all peptide pairs had formed parallel heterodimers (Fig. 3). No coiled coil assembly was seen within this time frame when the simulations were started with the peptides aligned in an anti-parallel orientation. Moreover, Asn pairing via hydrogen bonding could also be observed, supporting that Asn will guide the peptides

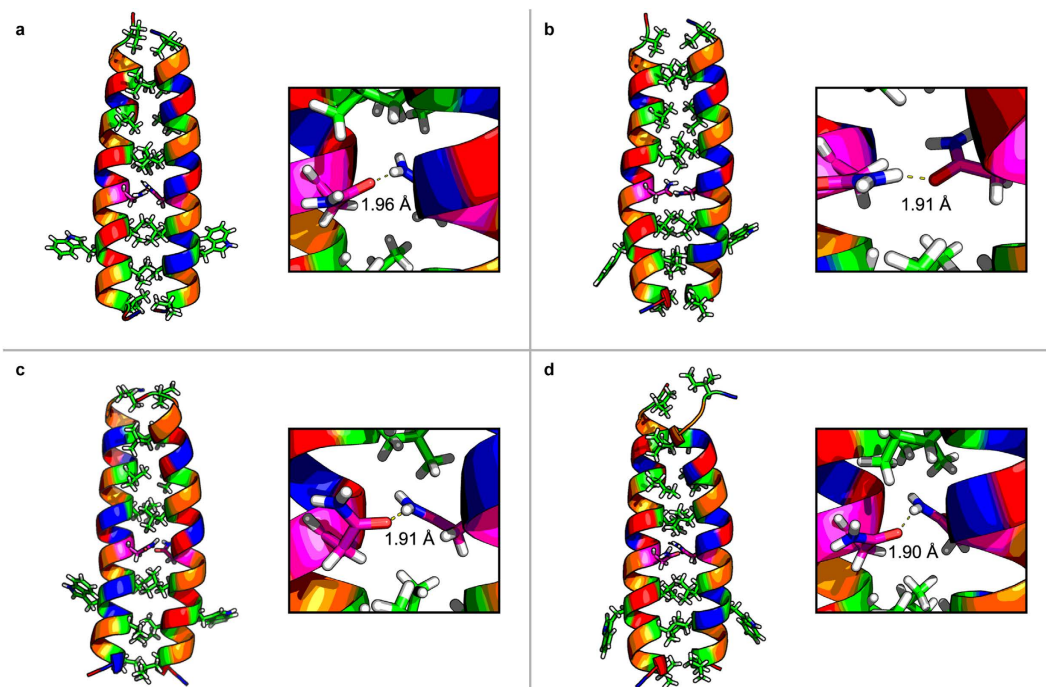


**Figure 3. Molecular dynamics simulations of (a) EVKV, (b) EVKI, (c) EIKV and (d) EIKI, showing formation of parallel heterodimeric coiled coils.** EIKI showed the tightest packing of the residues in the hydrophobic core of all four coiled coils, as indicated by the shorter hydrogen bond length for Asn-Asn'. Amino acids are coloured according to Lesk Scheme<sup>45</sup>.

to dimerize in a parallel orientation and in-register. The Asn-Asn' hydrogen bond distance was 1.96 Å in EVKV and 1.90 Å in EIKI. For EVKI and EIKV this distance was 1.91 Å in both peptide pairs. This agrees well with the CD data since a shorter hydrogen bond distance indicates a more tightly packed and stable dimer structure.

The dissociation constants ( $K_d$ ) for all heterodimers were estimated from thermal denaturation data recorded at different peptide monomer concentrations.  $T_m$  values were estimated and related to  $K_d$  (Supplementary Figure S5)<sup>33</sup>. The lowest  $K_d$  value at 20 °C was obtained for EIKI ( $K_d < 0.1$  nM), whereas EVKV showed significantly lower affinity for heterodimerization ( $K_d = 1.4$  μM). EVKI and EIKV had  $K_d$  values in the nanomolar range, 85 and 72 nM, respectively. By changing from Val-Val' at *d* in the hydrophobic core to Val-Ile' it is thus possible to increase the affinity for dimerization by a factor of ~20. In contrast, using Ile-Ile' pairing the affinity for heterodimerization was increased by more than four orders of magnitude as compared to Val-Val'.

**Temperature dependent self-sorting.** The peptides are obviously promiscuous since no negative design elements have been introduced to prevent formation of any of the four possible heterodimers. Moreover, all heterodimers display reasonably low dissociation constants, albeit spanning over a wide range. Because of the large differences in affinities for heterodimerization, the peptides are expected to undergo thermodynamic self-sorting when all of them are mixed. To investigate this hypothesis, EV, KV, EI and KI were mixed at different molar ratios and the thermal stability of the ensemble was characterized using CD spectroscopy. The total peptide concentration was kept constant at 50 μM and the ratios for EV:KV and EI:KI was kept at 1:1, respectively. Instead the relative mole percent ( $\chi_{\%}$ ) of [EI:KI] compared to [EV:KV] was varied from 0 to 100%. Since the different dimers have defined melting temperatures the number of transitions in the thermal denaturation curve of the mixtures reflects the number of different dimers present. Increasing the  $\chi_{\%}$  of [EI:KI] at 20 °C indeed increased the overall helicity and  $[\Theta]_{222}/[\Theta]_{208}$  ratio (Fig. 4a, Supplementary Table S3). This is expected because of the relative higher concentration of EIKI dimers formed. Increasing the  $\chi_{\%}$  of [EI:KI] also resulted in a higher overall thermal stability of the ensemble (Fig. 4b, Supplementary Table S3).

The degree of unfolding for different ratios was estimated by normalizing the denaturation curves using a two-state unfolding model (Fig. 4c). In the span from  $\chi_{10\%}$  to  $\chi_{90\%}$ , two major visible thermal transitions were obtained, one in the lower temperature span (<50 °C) and one in the higher (>80 °C), corresponding to the unfolding of EVKV and EIKI heterodimers, respectively. From the derivative of the thermal denaturation curves the presence of only two thermal unfolding transitions is clearly seen (Supplementary Figure S6). Computer simulations based on the  $K_d$  values of the dimers at different temperatures showed the same trend as well with only two thermal unfolding transitions (Fig. 4d).

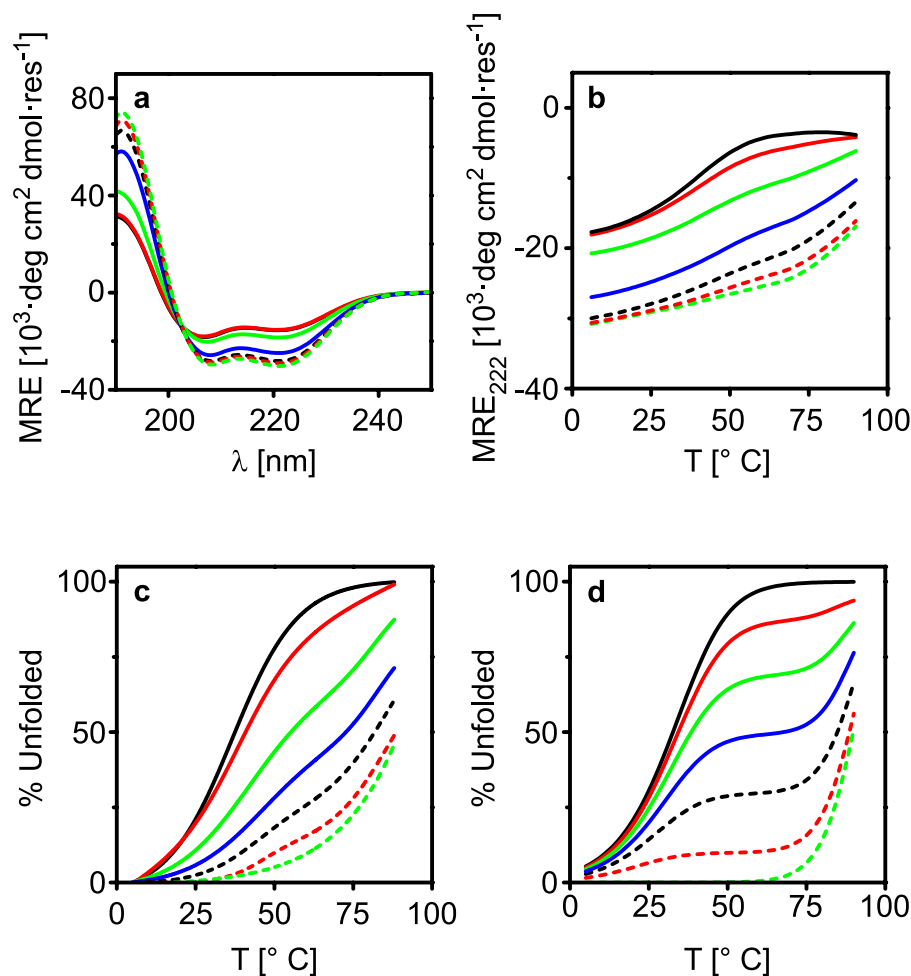


**Figure 4.** (a) CD spectra at 20 °C for different  $\chi_{\%}$  [EI:KI]. (b) Thermal denaturation curves for different  $\chi_{\%}$  [EI:KI]. (c) Normalized thermal denaturation curves for different  $\chi_{\%}$  [EI:KI] showing the % of unfolding and (d) % of unfolding obtained from simulations for different  $\chi_{\%}$  [EI:KI] and temperatures. Key:  $\chi_{0\%}$  [EI:KI] = black, solid;  $\chi_{10\%}$  [EI:KI] = red, solid;  $\chi_{30\%}$  [EI:KI] = green, solid;  $\chi_{50\%}$  [EI:KI] = blue, solid;  $\chi_{70\%}$  [EI:KI] = black, dash;  $\chi_{90\%}$  [EI:KI] = red, dash;  $\chi_{100\%}$  [EI:KI] = green, dash.

From computer simulations of all dimer combinations (Fig. 5a and Supplementary Figure S8) it is evident that the peptides predominantly assemble into EVKV and EIKI. A certain amount of EVKI and EIKV forms as well but at  $\chi_{50\%}$  and 20 °C to a very small extent, less than 2% of all dimers. Increasing the temperature above  $T_m$  for EVKV leads to an increase in the concentration of free EV and KV monomers. The concentration of EIKI stays fairly constant at temperatures below 60 °C because of the high thermal stability of this heterodimer. The low concentration of free EI and KI monomers thus prevents formation of EVKI and EIKV. Above 75 °C EIKI will start to dissociate to a larger extent. The resulting increase in concentration of free EI and KI will thus slightly increase the probability for formation of EVKI and EIKV heterodimers. At the same time the corresponding  $K_d$  values is relatively high under these conditions ( $>0.2 \mu\text{M}$  at 75 °C) and the concentration of these heterodimers will hence be low. Since EIKI has about two orders of magnitude lower  $K_d$  at this temperature, more than 92% of all dimers will be in the form of EIKI. By keeping the temperature fixed and instead varying the ratio of [EI:KI] to [EV:KV] it would in theory be possible to tune the relative equilibrium dimer concentrations (Fig. 5b). For example, at about  $\chi_{42\%}$  of [EI:KI] at 20 °C there will be equal concentrations of EVKV and EIKI heterodimers in a peptide mixture.

To further experimentally verify that the peptides undergo thermodynamic self-sorting we modified EV at the N-terminus with a fluorescent dye (Cy5). Although not considered very environmentally sensitive, cyanine dyes tethered to the terminus of single-stranded DNA display significant changes in fluorescence quantum yield, emission lifetime, and fluorescence anisotropy decay upon hybridization with a complementary DNA strand<sup>34,35</sup>. Addition of KI (5  $\mu\text{M}$ ) to EV-Cy5 (5  $\mu\text{M}$ ) resulted in increased emission intensity due to formation of (EV-Cy5)KI heterodimer (Fig. 6a,b). Subsequent addition of EI (5  $\mu\text{M}$ ) resulted in a drop in emission intensity, close to the original intensity of the monomeric EV-Cy5. Since KI has a significantly higher affinity for EI than for EV, the addition of EI leads to a transition from

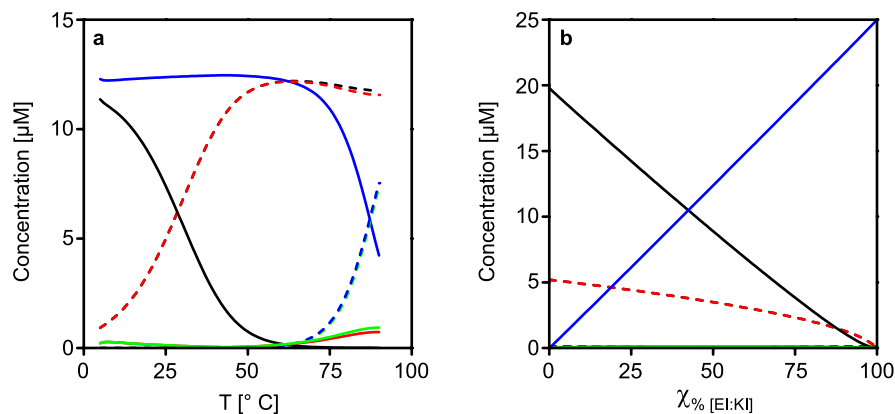


**Figure 5.** (a) Simulations of  $\chi_{50\%}$  [EI:KI] as a function of temperature. At 20°C the monomers self-sort into predominantly EVKV and EIKI and only 2% forms EVKI or EIKV dimers. (b) Simulated equilibrium concentrations of monomers and heterodimers when varying  $\chi_{\%}$  [EI:KI] at 20°C. The relative amount of EVKV and EIKI will be roughly the same at  $\chi_{42\%}$  [EI:KI]. For other  $\chi_{\%}$  [EI:KI], see supporting information. Key: EV = black, dash; KV = red, Dash; EI = green, dash; KI = blue, dash; EVKV = black, solid; EVKI = red, solid; EIKV = green, solid; EIKI = blue, solid.

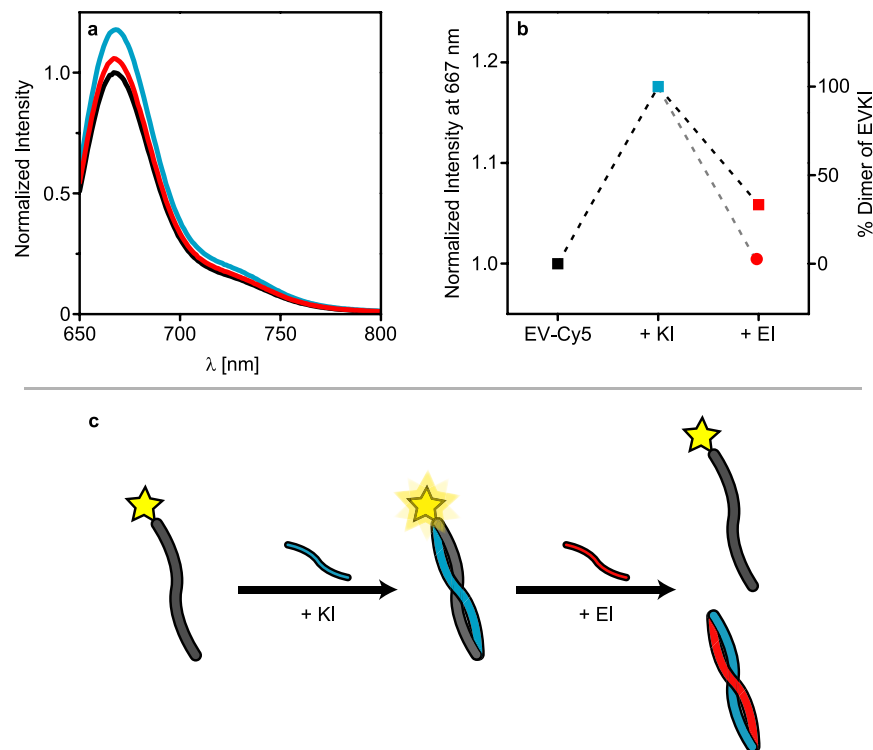


**Figure 6.** (a) Fluorescence spectra and (b) change in normalized intensity at 667 nm for EV-Cy5 upon addition of EI and KI. Addition of the complementary peptide KI, thus forming EVKI dimers, results in an increase in fluorescence intensity. Subsequent addition of EI reduces the fluorescence intensity due to formation of EIKI dimers, leaving free EV-Cy5. The experimental data correlate well with simulations. (c) Schematic representation of the experiment. Key: (a) EV-Cy5 = black, solid; +KI = blue, solid; +EI = red, solid. (b) EV-Cy5 = black, square; +KI = blue, square; +EI = red, square; (simulation) +EI = red, circle.

(EV-Cy5) KI to EIKI heterodimers and EV-Cy5 monomers as illustrated in Fig. 6c. This change in binding partner was also supported by simulations (Fig. 6b). The smaller amount of monomeric EV-Cy5 seen in the experiment after addition of EI is presumably an effect of the kinetics involved in the exchange of partners in the heterodimer. The simulations were run until equilibrium whereas the experimental data was acquired after 30 minutes incubation and the exchange was likely not fully completed within

this time frame. Addition of EI prior to KI, but under otherwise identical conditions, instead resulted in a slight decrease in fluorescence intensity similar to the photo-bleaching of the dye upon acquisition of repeated spectra (Supplementary Figure S7).

## Conclusions

By using only four different de novo designed peptides it is possible to obtain four different parallel coiled coil heterodimers. Their dissociation constants span from micromolar to picomolar at room temperature and because of the large difference in affinities, the peptides undergo thermodynamic social self-sorting when combined. Predominately two out of four possible heterodimers were formed, as shown by thermal denaturation curves of different peptide combinations, along with fluorescence data and simulations. In previous work, self-sorting has primarily been imposed by introducing negative design elements to generate fully orthogonal peptide sequences. In contrast, the peptides described here are not designed to exclude certain combinations of heterodimers based on unfavourable interactions and all four heterodimers can thus form. The possibility to form defined heterodimers with high fidelity from mixtures of non-orthogonal peptides can facilitate efforts to realize defined complex polypeptide nanostructures. The distinct self-sorting properties of the peptide heterodimers presented here will thus be a valuable addition to the rich toolbox of coiled coil peptides available in the literature. Furthermore, the possibility to tune the strength of association by different hydrophobic core packing and the fact that they undergo social self-sorting makes these peptides highly attractive supramolecular building blocks in dynamic peptide-based nanomaterials. The wide range of affinities opens possibilities to tune materials properties with high precision, which can be used for e.g. fabrication of peptide-based hydrogels with defined viscoelastic properties for tissue engineering, 3D cell culturing and drug delivery, and for tuneable self-assembly of peptide-nanoparticle hybrids for sensing applications.

## Methods

**General.** Fmoc-protected amino acids were purchased from Iris Biotech GmbH. HCTU and DIPEA were acquired from Protein Technologies, Inc. DMF and acetonitrile were obtained from VWR International. All other chemicals were acquired from Sigma Aldrich. All measurements were carried out in phosphate buffer (PB; mono- and disodium phosphate, total concentration 10 mM) and adjusted to pH 7 using phosphoric acid or sodium hydroxide. Peptide concentrations were determined by UV absorbance ( $\epsilon_{280}(\text{Trp}) = 5690 \text{ M}^{-1} \text{ cm}^{-1}$ ). All measurements were at 50  $\mu\text{M}$  total peptide concentration unless otherwise noticed. All samples were allowed to equilibrate for 30 min after mixing before measurement.

**Peptide Synthesis and purification.** The peptides were obtained by solid phase peptide synthesis on a Symphony Quartet from Protein Technologies, Inc. As solid phase H-Rink-Amide ChemMatrix resin (0.47 mmol of  $\text{NH}_2/\text{g}$  of resin) was used on a 100  $\mu\text{M}$  scale. Synthesis was performed using a standard Fmoc protocol with a 6-fold molar excess of amino acids and HCTU as coupling agent. N-terminal acetylation was carried out in acetic anhydride/DMF (1:1). For peptides used in fluorometric measurements Cy5-NHS was used instead of acetic anhydride at this step. The peptides were cleaved from the resin with mixtures of trifluoroacetic acid (TFA)/triisopropylsilane/water (95:2.5:2.5, 90 min). Peptides were filtered from the resin and the TFA/peptide mixture was concentrated to approximately 1 ml under a flow of nitrogen. The crude peptides were then precipitated in  $-20^\circ\text{C}$  cold diethyl ether and isolated by centrifugation and subsequently thoroughly washed. The isolated product were dissolved in 1:1 acetonitrile/water and lyophilized to a dry powder.

Purification was done by reverse phase HPLC using a preparative Kromatek HiQ-Sil C18HS column (250 by 21.1 mm) on a Dionex Ultimate 3000 LC system from Thermo Scientific. Depending on sequence different buffers were used. Peptides with a positive net charge (K-peptides) were purified by running linear gradients of water and acetonitrile (Buffer A, 90% water, 9.9% acetonitrile and 0.1% TFA; Buffer B, 10% water, 89.9% acetonitrile and 0.1% TFA). Peptides with a negative net charge (E-peptides) were purified by running linear gradients of triethylammonium acetate buffer (TEAA-buffer, 20 mM triethylamine, 20 mM acetic acid, adjusted to pH 9) and acetonitrile (Buffer C, 90% TEAA-buffer, 10% acetonitrile; Buffer D, 10% TEAA-buffer, 90% acetonitrile). Linear gradients were from 10% to 40% buffer B or D during 8.5 min with a constant flowrate of 20 ml/min. All peptides were monitored and collected based on UV-signal at 229 nm and 274 nm. Final purity was controlled by reverse phase HPLC and the mass identity was confirmed by MALDI-ToF mass spectrometry with  $\alpha$ -cyano-4-hydroxycinnamic acid as matrix.

**Circular Dichroism (CD) Spectroscopy.** CD spectra and thermal denaturation curves were recorded using a Chirascan<sup>TM</sup> spectropolarimeter from Applied Photophysics with a TC 125 temperature controller from Quantum Northwest. CD spectra were measured between 190 and 250 nm at  $20^\circ\text{C}$  in quartz cuvettes with a step size of 0.5 nm. Thermal curves were measured by heating from 5 to  $90^\circ\text{C}$  at  $1^\circ\text{C}$  intervals with  $0.2^\circ\text{C}$  accuracy and at a rate of roughly  $50^\circ\text{C}$  per hour. The CD signal at 222 nm was recorded for each temperature. These curves were fitted to either a mono- or biphasic sigmoidal function depending on whether one or two transitions was observed, and corresponding melting temperatures were estimated from these. Each CD experiment was run in triplicates and data was averaged and



converted to mean residue ellipticity (MRE,  $[\Theta]$ ). Normalization of ratio thermal denaturation curves was done by using equation (1).

$$\%_{\text{unfold}} = \left( 1 - \left( \frac{[\Theta] - [\Theta]_{\text{monomer}}}{[\Theta]_{\text{F}}} \right) \right) \times 100 \quad (1)$$

that is a modified version of Litowski and Hodges<sup>36</sup>.  $[\Theta]$  is the measured MRE at 222 nm and  $[\Theta]_{\text{monomer}}$  is the estimated MRE at 222 nm in a mixture of monomers if no interaction occur between them. These value are estimated from thermal denaturation experiments of the monomers.  $[\Theta]_{\text{F}}$  is the MRE at maximum folding, for simplification estimated as the value of  $([\Theta] - [\Theta]_{\text{monomer}})$  at 5 °C. When  $[\Theta] = [\Theta]_{\text{monomer}}$  it is assumed that complete unfolding has occurred.

**Molecular dynamics simulations.** Simulations were performed using the GROMACS package<sup>37</sup>. The overall temperature of the water and peptides was kept constant, coupling each group of molecules independently at 300 K with a V-rescale thermostat<sup>38</sup>. The pressure was coupled to a Parrinello-Rahman<sup>39,40</sup> barostat at 1 atm separately in every dimension. The temperature and pressure time constants of the coupling were 0.1 and 2 ps, respectively. Integration of equations of motion was performed by using a leap frog algorithm with a time step of 2 fs. Periodic boundary conditions were implemented in all systems. A cut-off of 1 nm was implemented for the Lennard-Jones and the direct space part of the Ewald sum for Coulombic interactions. The Fourier space part of the Ewald splitting was computed by using the particle-mesh-Ewald method<sup>41</sup>, with a grid length of 0.16 nm on the side and a cubic spline interpolation. TIP3P water model<sup>42</sup> was used and the peptide parameters were from the CHARMM force field<sup>43,44</sup>.

**Self-sorting simulations.** Simulations were carried out using MATLAB R2014b (The MathWorks, Inc.). Details, including scripts, can be found in supplementary information.

## References

1. Crick, F. H. C. The packing of  $\alpha$ -helices: simple coiled-coils. *Acta Crystallogr.* **6**, 689–697 (1953).
2. Kim, P. S., Berger, B. & Wolf, E. MultiCoil: A program for predicting two-and three-stranded coiled coils. *Protein Sci.* **6**, 1179–1189 (1997).
3. Pauling, L. & Corey, R. B. Compound helical configurations of polypeptide chains: structure of proteins of the alpha-keratin type. *Nature* **171**, 59–61 (1953).
4. Woolfson, D. N. in *Adv. Protein Chem.* Vol. Volume 70 (eds David, A. D. Parry & John, M. Squire) 79–112 (Academic Press, 2005).
5. Mason, J. M. & Arndt, K. M. Coiled Coil Domains: Stability, Specificity, and Biological Implications. *ChemBiochem* **5**, 170–176 (2004).
6. Hodges, R. S. De novo design of  $\alpha$ -helical proteins: basic research to medical applications. *Biochem. Cell Biol.* **74**, 133–154 (1996).
7. Yu, Y. B. Coiled-coils: stability, specificity, and drug delivery potential. *Adv. Drug Deliv. Rev.* **54**, 1113–1129 (2002).
8. Parry, D. A. D., Fraser, R. D. B. & Squire, J. M. Fifty years of coiled-coils and  $\alpha$ -helical bundles: A close relationship between sequence and structure. *J. Struct. Biol.* **163**, 258–269 (2008).
9. Versluis, F. *et al.* In Situ Modification of Plain Liposomes with Lipidated Coiled Coil Forming Peptides Induces Membrane Fusion. *J. Am. Chem. Soc.* **135**, 8057–8062 (2013).
10. Kaplan, J. B., Reinke, A. W. & Keating, A. E. Increasing the affinity of selective bZIP-binding peptides through surface residue redesign. *Protein Sci.* **23**, 940–953 (2014).
11. Mehrban, N. *et al.* Assessing Cellular Response to Functionalized  $\alpha$ -Helical Peptide Hydrogels. *Adv. Healthcare Mater.* **3**, 1387–1391 (2014).
12. Jing, P., Rudra, J. S., Herr, A. B. & Collier, J. H. Self-Assembling Peptide-Polymer Hydrogels Designed From the Coiled Coil Region of Fibrin. *Biomacromolecules* **9**, 2438–2446 (2008).
13. Oshaben, K. M. & Horne, W. S. Tuning Assembly Size in Peptide-Based Supramolecular Polymers by Modulation of Subunit Association Affinity. *Biomacromolecules* **15**, 1436–1442 (2014).
14. Stevens, M. M., Flynn, N. T., Wang, C., Tirrell, D. A. & Langer, R. Coiled-Coil Peptide-Based Assembly of Gold Nanoparticles. *Adv. Mater.* **16**, 915–918 (2004).
15. Gradišar, H. *et al.* Design of a single-chain polypeptide tetrahedron assembled from coiled-coil segments. *Nat. Chem. Biol.* **9**, 362–366 (2013).
16. Fletcher, J. M. *et al.* Self-Assembling Cages from Coiled-Coil Peptide Modules. *Science* **340**, 595–599 (2013).
17. Lowik, D. W. P. M., Leunissen, E. H. P., van den Heuvel, M., Hansen, M. B. & van Hest, J. C. M. Stimulus responsive peptide based materials. *Chem. Soc. Rev.* **39**, 3394–3412 (2010).
18. Zaccari, N. R. *et al.* A de novo peptide hexamer with a mutable channel. *Nat. Chem. Biol.* **7**, 935–941 (2011).
19. Monera, O. D., Kay, C. M. & Hodges, R. S. Electrostatic Interactions Control the Parallel and Antiparallel Orientation of  $\alpha$ -Helical Chains in Two-Stranded  $\alpha$ -Helical Coiled-Coils. *Biochemistry* **33**, 3862–3871 (1994).
20. Zhu, B.-Y., Zhou, M. E., Kay, C. M. & Hodges, R. S. Packing and hydrophobicity effects on protein folding and stability: Effects of  $\beta$ -branched amino acids, valine and isoleucine, on the formation and stability of two-stranded  $\alpha$ -helical coiled coils/leucine zippers. *Protein Sci.* **2**, 383–394 (1993).
21. Thomas, F., Boyle, A. L., Burton, A. J. & Woolfson, D. N. A Set of de Novo Designed Parallel Heterodimeric Coiled Coils with Quantified Dissociation Constants in the Micromolar to Sub-nanomolar Regime. *J. Am. Chem. Soc.* **135**, 5161–5166 (2013).
22. Zhang, R., Yang, J., Chu, T.-W., Hartley, J. M. & Kopeček, J. Multimodality Imaging of Coiled-Coil Mediated Self-Assembly in a “Drug-Free” Therapeutic System. *Adv. Healthcare Mater.* **4**, 1054–1065 (2015).
23. Akey, D. L., Malashkevich, V. N. & Kim, P. S. Buried Polar Residues in Coiled-Coil Interfaces†. *Biochemistry* **40**, 6352–6360 (2001).
24. Gradišar, H. & Jerala, R. De novo design of orthogonal peptide pairs forming parallel coiled-coil heterodimers. *J. Pept. Sci.* **17**, 100–106 (2011).
25. Litowski, J. R. & Hodges, R. S. Designing Heterodimeric Two-stranded  $\alpha$ -Helical Coiled-coils: Effects of hydrophobicity and  $\alpha$ -helical propensity on protein folding, stability, and specificity. *J. Biol. Chem.* **277**, 37272–37279 (2002).

26. Harbury, P. B., Zhang, T., Kim, P. S. & Alber, T. A switch between two-, three-, and four-stranded coiled coils in GCN4 leucine zipper mutants. *Science* **262**, 1401–1407 (1993).
27. O’Shea, E. K., Rutkowski, R. & Kim, P. S. Mechanism of specificity in the Fos-Jun oncoprotein heterodimer. *Cell* **68**, 699–708 (1992).
28. Lau, S. Y., Taneja, A. K. & Hodges, R. S. Synthesis of a model protein of defined secondary and quaternary structure. Effect of chain length on the stabilization and formation of two-stranded alpha-helical coiled-coils. *J. Biol. Chem.* **259**, 13253–13261 (1984).
29. Holtzer, M. E. & Holtzer, A. Alpha-helix to random coil transitions: determination of peptide concentration from the CD at the isodichroic point. *Biopolymers* **32**, 1675–1677 (1992).
30. Vincent, T. L., Green, P. J. & Woolfson, D. N. LOGICOIL—multi-state prediction of coiled-coil oligomeric state. *Bioinformatics* **29**, 69–76 (2013).
31. Li, C., Wang, X.-F., Chen, Z., Zhang, Z. & Song, J. Computational characterization of parallel dimeric and trimeric coiled-coils using effective amino acid indices. *Mol. BioSyst.* **11**, 354–360 (2015).
32. Mahrenholz, C. C., Abfalder, I. G., Bodenhofer, U., Volkmer, R. & Hochreiter, S. Complex Networks Govern Coiled-Coil Oligomerization – Predicting and Profiling by Means of a Machine Learning Approach. *Mol. Cell. Proteomics* **10**, doi: 10.1074/mcp.M110.004994 (2011).
33. Marky, L. A. & Breslauer, K. J. Calculating thermodynamic data for transitions of any molecularity from equilibrium melting curves. *Biopolymers* **26**, 1601–1620 (1987).
34. Agbaywe, C. & Somoza, M. M. Sequence-Dependent Fluorescence of Cyanine Dyes on Microarrays. *PLoS ONE* **6**, e22177 (2011).
35. Sanborn, M. E., Connolly, B. K., Gurunathan, K. & Levitus, M. Fluorescence Properties and Photophysics of the Sulfoindocyanine Cy3 Linked Covalently to DNA. *J. Phys. Chem. B* **111**, 11064–11074 (2007).
36. Litowski, J. R. & Hodges, R. S. Designing heterodimeric two-stranded  $\alpha$ -helical coiled-coils: the effect of chain length on protein folding, stability and specificity. *J. Pept. Res.* **58**, 477–492 (2001).
37. Van Der Spoel, D. *et al.* GROMACS: Fast, flexible, and free. *J. Comput. Chem.* **26**, 1701–1718 (2005).
38. Bussi, G., Donadio, D. & Parrinello, M. Canonical sampling through velocity rescaling. *J. Chem. Phys.* **126**, 014101 (2007).
39. Parrinello, M. & Rahman, A. Polymorphic transitions in single crystals: A new molecular dynamics method. *J. Appl. Phys.* **52**, 7182–7190 (1981).
40. Nosé, S. & Klein, M. L. Constant pressure molecular dynamics for molecular systems. *Mol. Phys.* **50**, 1055–1076 (1983).
41. Darden, T., York, D. & Pedersen, L. Particle mesh Ewald: An  $N \cdot \log(N)$  method for Ewald sums in large systems. *J. Chem. Phys.* **98**, 10089–10092 (1993).
42. Jorgensen, W. L., Chandrasekhar, J., Madura, J. D., Impey, R. W. & Klein, M. L. Comparison of simple potential functions for simulating liquid water. *J. Chem. Phys.* **79**, 926–935 (1983).
43. MacKerell, A. D. *et al.* All-Atom Empirical Potential for Molecular Modeling and Dynamics Studies of Proteins†. *J. Phys. Chem. B* **102**, 3586–3616 (1998).
44. Mackerell, A. D., Jr., Feig, M. & Brooks, C. L. 3rd. Extending the treatment of backbone energetics in protein force fields: limitations of gas-phase quantum mechanics in reproducing protein conformational distributions in molecular dynamics simulations. *J. Comput. Chem.* **25**, 1400–1415 (2004).
45. Lesk, A. M. *Introduction to bioinformatics*. 1st edn (Oxford University Press, 2002).

## Acknowledgments

This work was supported by the Swedish Research Council (VR), and the Swedish Foundation for Strategic Research (SSF). During this study C.A. was enrolled in the graduate school Forum Scientium.

## Author Contributions

D.A. suggested and supervised the work. C.A. and S.D. designed and synthesised the peptides. C.A. acquired and analysed the CD data. F.Z. and H.S. did the MD-simulations. P.Ö. did the MATLAB scripts and simulations with C.A. C.A. did the fluorescence measurements and K.E. and D.A. assisted with analysis of acquired data. C.A. and D.A. wrote the paper with input from all authors.

## Additional Information

**Supplementary information** accompanies this paper at <http://www.nature.com/srep>

**Competing financial interests:** The authors declare no competing financial interests.

**How to cite this article:** Aronsson, C. *et al.* Self-sorting heterodimeric coiled coil peptides with defined and tuneable self-assembly properties. *Sci. Rep.* **5**, 14063; doi: 10.1038/srep14063 (2015).



This work is licensed under a Creative Commons Attribution 4.0 International License. The images or other third party material in this article are included in the article’s Creative Commons license, unless indicated otherwise in the credit line; if the material is not included under the Creative Commons license, users will need to obtain permission from the license holder to reproduce the material. To view a copy of this license, visit <http://creativecommons.org/licenses/by/4.0/>